

RSC Advances



This is an *Accepted Manuscript*, which has been through the Royal Society of Chemistry peer review process and has been accepted for publication.

Accepted Manuscripts are published online shortly after acceptance, before technical editing, formatting and proof reading. Using this free service, authors can make their results available to the community, in citable form, before we publish the edited article. This *Accepted Manuscript* will be replaced by the edited, formatted and paginated article as soon as this is available.

You can find more information about *Accepted Manuscripts* in the [Information for Authors](#).

Please note that technical editing may introduce minor changes to the text and/or graphics, which may alter content. The journal's standard [Terms & Conditions](#) and the [Ethical guidelines](#) still apply. In no event shall the Royal Society of Chemistry be held responsible for any errors or omissions in this *Accepted Manuscript* or any consequences arising from the use of any information it contains.

Synergy Between Pd and Au in Pd-Au(100) Bimetallic Surface For Water Gas Shift Reaction. A DFT Study

Muhammad Adnan Saqlain^{1,2}, Akhtar Hussain^{3,4}, Muhammad Siddiq^{1*}, Alexandre A. Leitão^{2*}*

1. Department of Chemistry, Quaid-i-Azam University, Islamabad, 45320, Pakistan

2. Departamento de Química, Universidade Federal de Juiz de Fora, Juiz de Fora, MG, CEP 36036 -330, Brazil

3. TPD, Pakistan Institute of Science and Technology, PINSTECH, P. O. Nilore, Islamabad, Pakistan.

4. National Centre for Physics, Islamabad, Pakistan

** Corresponding Author*

Akhtar Hussain, TPD, Pakistan Institute of Science and Technology, PINSTECH, P. O. Nilore, Islamabad, Pakistan

Email. ahmohal@yahoo.com

Muhammad Siddiq, Department of Chemistry, Quaid-i-Azam University, Islamabad, 45320, Pakistan

Email; m_sidiq12@yahoo.com

Abstract

Density Functional Theory calculations were performed to model a reaction relevant bimetallic surface and study water gas shift reaction. It was found that in vacuum, Pd prefers to stay in the bulk due to more negative formation energies. However, strong CO-philic nature of Pd causes surface segregation of Pd a relevant process, with segregation energy increasing linearly with number of Pd atoms segregated. Therefore, it is expected that under CO rich environments, Pd covered Au will be the relevant structure of the Pd-Au bimetallic surface. The surface is highly active for water dissociation and subsequent reactions leading to CO oxidation. Based on our results, it is predictable that the adsorbed carboxyl pathway will dominate the kinetics. Our results show that H₂ adsorbs dissociatively on this surface which opens new channels for research regarding candidature of such model surfaces as hydrogen storage materials. An important consequence of our results is that these guide into selective development of alloy surfaces keeping in view the adsorbate induced surface segregations.

Key words: - Segregation, water dissociation, synergy, water gas shift reaction, density functional theory

1. Introduction

Adsorption, desorption, dissociation, aggregation and formation of water on metals is of particular interest for many chemical processes,¹⁻⁴ therefore, interaction of water with solids has been one of the hot areas of research. Water gas shift reaction, $\text{CO} + \text{H}_2\text{O} \rightarrow \text{CO}_2 + \text{H}_2$, is one of important industrial processes leading to H₂ production.¹⁻⁴ Being exothermic, low temperature favors the reaction in forward direction. However, due to kinetic restrictions, the temperature is kept a little higher. Hence, it is desirable to have low temperature shift catalysts with superior reaction rates. Bimetallic surfaces are one of promising candidate materials for better catalytic performance.

Structure, morphology, composition, size and shape of the catalyst (nanoparticles) are the descriptors that determine the performance of a catalyst. Optimum catalytic properties of a surface can be realized by appropriately architecting its structure and composition⁵. Due to flexibility in composition and distinct arrangement of atoms than the pure metals, bimetallic surfaces (alloys) are superior combination of counterparts and provide a better way to control the

properties and electronic structure of catalyst.⁶⁻⁹ The need to concoct catalysts with well-defined structure and controllable properties at the nanoscale level made bimetallic surfaces a hot area of research. Better catalytic performance of bimetallic surfaces has been explained in terms of ensemble and ligand effects.^{10,11}

Since the discovery of superior catalytic performance of Au nanoparticles for CO oxidation^{12,13}, there has been a robust research in Au based catalysts, nevertheless, our previous investigation has shown that water dissociation is very difficult on pure Au under low temperature conditions¹⁴. Since dissociation of water is the rate limiting step on pure Au¹⁴ and Cu¹⁵ surfaces; therefore, alternate shift catalysts are being examined. As CO oxidation is much easier on Au^{12,13}, therefore, the counterpart metal should actively dissociate water. Such a combination of Au and ad-metal will have cooperative effect both in catalyzing water dissociation and consequently in CO oxidation. In our model of bimetallic surfaces, we have examined Pd modified Au bimetallic surface for water dissociation and CO oxidation.

Since Au and Pd are completely miscible, several forms of Au-Pd systems¹⁶⁻¹⁹ have been studied for a variety of reactions including vinyl acetate synthesis²⁰⁻²², alcohol oxidation²³, H₂O₂ formation²⁴, CO oxidation^{17,25-27} and oxygen reduction reactions^{28,29}. Several theoretical and experimental studies have been dedicated to evaluate the structure and composition of Au-Pd systems.³⁰⁻³⁶ Motivated by synergy between Au-Pd for above mentioned reactions and its better performance than single metal surfaces, we explored its potential application in water gas shift reaction, an area where, Au-Pd system has not yet been investigated. Our findings regarding water gas shift reaction are presented in this work.

2. Computational details

All the calculations were performed in plane waves basis set using VASP.^{37,38} Plane-waves with a kinetic energy below or equal to 400 eV were included in the calculations, the convergence criterion for forces being 0.05 eV/Å. The projected augmented wave (PAW) potential was employed to accommodate ion-electron interactions³⁹ while the exchange correlation energy was calculated by GGA-PW91 approximation.^{40,41}

Bimetallic surface was represented with slab model. All the slabs consist of 4 layers in which the top 2 layers were relaxed with a vacuum layer of $>10 \text{ \AA}$ to separate the periodic images. We have used $p(3\times 3)$ unit cell with the reciprocal space sampled with $(3\times 3\times 1)$ k-point meshes. Initially, the positions of Au atoms were frozen using optimized lattice parameter of 4.18 \AA , the experimental value being 4.08 \AA .³² Face-centered cubic (fcc) unit cell was used to calculate the lattice parameter and Monkhorst-Pack method⁴² was used to sample its reciprocal space with a $(15\times 15\times 15)$ k-point grid. Fractional occupancies were accommodated using first-order Methfessel-Paxton smearing-function having the width $\leq 0.1 \text{ eV}$.⁴³ For determination of minimum energy path (MEP), climbing-image nudged elastic band (cNEB) method was used.^{44,45} Confirmation of transition states (TS) was made by phonons calculations within the harmonic approximation. Only the Hessian matrix of the adsorbate was included in calculations neglecting the adsorbate-surface interaction.⁴⁶ Non-spin polarized calculations were performed for closed shell molecules at Γ point with $10\times 10\times 10 \text{ \AA}^3$ face-centred cubic unit cell. However, spin polarized calculations were performed for open shell species with a $10\times 12\times 14 \text{ \AA}^3$ orthorhombic unit cell.

3. Results and Discussion

i. Structure of Au-Pd bimetallic surface

Before calculating reaction barriers, we explored the stability of bimetallic surface with and without the adsorbents.

In principle, with or without adsorbates, Pd will either stay in the bulk or segregate to the surface. To know the relative thermodynamically stable configuration and the segregation energy with and without CO molecule, two separate surfaces were constructed, one with Pd in the subsurface layer and the other in which Pd occupies the top layer, a procedure which is well documented.⁴⁷⁻⁴⁹ The relative stable configuration can be predicted by calculating the formation energy according to equation⁴⁸ (1) below.

$$\Delta E_{\text{mix}} = E_{\text{Pd-Au/slab}} + nE_{\text{Au/bulk}} - nE_{\text{Pd/bulk}} - E_{\text{Au/slab}} \quad (1)$$

Where $E_{\text{Pd-Au/slab}}$ and $E_{\text{Au/slab}}$ refer to slab energy of Au-Pd and pure Au, respectively, while $E_{\text{Au/bulk}}$ and $E_{\text{Pd/bulk}}$ represent the energy of bulk Au and bulk Pd, respectively. n represents no of atoms of Au replaced by Pd.

----- Insert Figure 1 here -----

ΔE_{mix} was negative for both constitutions. In vacuum; however, Pd prefers to stay in the subsurface layer, due to negative formation energies (shown in Figure 1). Segregation of a single Pd atom from bulk to the surface layer destabilizes the system by 0.40 eV. Segregation of 2, 3 and 4 atoms from bulk to surface layer destabilizes the system by 0.83, 1.22 and 1.62 eV, respectively (Figure 1 a-h). Moreover, whether in the bulk or surface, formation of Pd dimer destabilizes the system by 0.49 and 0.53 eV, respectively (Figure 1 i-l). Thus, in vacuum, Pd prefers Au-Pd-Au bonds instead of Pd-Pd bonds. However, in presence of CO, the trend shifts altogether. In presence of CO, segregation of Pd from bulk to surface stabilizes the system by 0.1 and 0.32 eV, for 1 and 2 Pd atoms, respectively (Figure 1 m-p). While formation of contiguous Pd atoms is hindered in the vacuum; however, CO induces formation of contiguous Pd atoms. Thus for Pd in the surface layer, the system is stabilized by 0.43 eV for Pd-Pd bond formation over Au-Pd-Au bond formation, consistent with reported data.^{26,27,33,47,50} Finally, binding energy for a single molecule of CO on Pd covered Au is 1.5 eV higher than Pd in bulk. Therefore, it is expected that CO will induce surface segregation of Pd. Our observations regarding CO induced Pd segregation are consistent with experimental and theoretical observations. It has been demonstrated that in absence of any reactant, Pd prefers to stay in the bulk of Au-Pd alloy, however, in presence of CO, Pd segregates to the surface and the surface concentration of Pd on Au depends upon temperature and partial pressure of gas. If the binding energy of molecule is too low, it will hardly induce any segregation and therefore, no catalytic advantage of Pd on Au would be available.^{26,27,33,47,50} Similarly, NO has also been shown to induce segregation of Pd in a Pd-Au alloy, with no segregation in absence of NO and a large segregation in presence of NO, the surface layer being 82% rich in Pd after exposure to NO.³² A recent study reveals that, for Au based bimetallic surfaces, all the members of group 9, 10 and 11 tend to segregate to the surface upon CO adsorption.⁴⁹ This is very important from catalysis point of view, especially for CO oxidation. As CO induced surface segregations take place in Pd-Au alloy, therefore, to mimic the reaction relevant catalyst, Pd terminated surface was considered for further reactions.

----- Insert Table 1 here -----

ii. Adsorption of Water

Adsorption energies and corresponding geometries of water are shown in Table 1. and Figure 2 a-b. Linear coordination is the preferred adsorption configuration of water on Au-Pd surface. Water adsorbs through its O with H atoms parallel to the surface. Metal to O atom distance for Au-Pd is 2.38Å. Although bridge coordination is relatively less stable compared to top coordination (Au-Pd only); however, water is only activated when it coordinates at the bridge site. As the energy difference between top and bridge coordination is only marginal, diffusion of water on these two sites is energetically feasible, albeit, activation is only observed when coordinated on bridge site.

As cited above, structure of adsorbed water is more or less similar to gas phase molecule when it coordinates linearly. On the other hand, if coordinated on bridge site, HOH bond angle broadens significantly (108.8°) relative to gas phase molecule (104.5°).⁵¹ However, bond length does not alter to significant value, being more or less the same as in gas phase water molecule (0.98 Å).⁵¹

Adsorption of H₂O is associated with structural changes of the surface atoms. We observed that H₂O adsorption causes surface atoms to relax. We could observe lateral relaxation with negligible vertical relaxation. Surface atoms relax by 0.2Å relative to clean surface. (Figure 2. and Table 1.)

Experimentally and theoretically, it has been shown that water adsorbs molecularly on most of the surfaces with a minor binding energy. Our calculated binding energy of water on model bimetallic surface is similar to those reported ones.⁵²⁻⁵⁶ Moreover, binding energy of water as observed on bimetallic surface is higher than the counterpart monometallic surfaces. For example, the binding energy of H₂O on Au-Pd bimetallic surface is higher than Pd(111) surface, for which the E_{ads} of H₂O is -0.30 eV⁵³. Thus bimetallic surfaces not only adsorb water more strongly but also activate it leading to its easy disintegration into OH and H, as discussed in coming section.

iii. Adsorption of OH, H and O

Water dissociation leads to formation of OH, O and H species, therefore, the preferred binding sites and binding geometries of these intermediates were screened first. For OH radicals, adsorption at hollow site is stable adsorption configuration with binding energy of -3.02 eV where as metal to O distance is 2.33 Å. Like water adsorption, OH adsorption also induces

relaxation of surface atoms. **Table 1** shows the relaxation of surface atoms induced by OH coordination at its preferred adsorption site. Adsorption energy of OH is similar to reported values on other surfaces.^{8,14,15,52,53,55,57,58}

H tends to adsorb more strongly on bridge site with E_{ads} of -2.81 eV, the metal to H distance being 1.72 Å. Adsorption of H is associated with shrinking of surface atoms. Table 1 lists numeric values of this contraction of surface atoms by H adsorption. E_{ads} of H on bimetallic surface is consistent with literature values on different surfaces.^{8,14,53,55,57-60}

O prefers hollow (-4.39 eV) site on Au-Pd surface. Diffusion of O from bridge to hollow site is probable. Metal to O distance was calculated as 2.17 Å, consistent with observations of Yuan & Liu for Pd cluster on Au cluster.¹⁷

iv. Co-adsorption of OH and H

Co-adsorption of OH-H is the final state of dissociated water. For this, several possible co-adsorption configurations were scanned. However, OH and H prefer bridge-bridge coordination (Figure 2 d) with adsorption energy of -5.81 eV. Surface atoms relax upon co-adsorption of OH and H, for which Table 1. lists the relaxation induced by these species on the bimetallic surface along with metal to O/H distances. Compared to individually adsorbed OH and H on separate unit cells, the co-adsorption is slightly repulsive (0.03 eV).

v. Co-adsorption of O and H

OH radicals produced from water dissociation disintegrate in two ways, the dissociation of OH radicals to O and H and the disproportionation of OH radicals to produce O and H₂O.

Bridge-bridge coordination of O and H is the most stable co-adsorbed configuration (the FS of OH dissociation), with adsorption energy of -6.61 eV. See Table 1. for metal to O/H distance and relaxation of surface atoms due to co-adsorption of O and H. Contrary to co-adsorption of OH and H, co-adsorption of O-H is significantly repulsive (0.60 eV).

vi. Co-adsorption of 2 OH groups and H₂O and O

Co-adsorption of 2 OH radicals and H₂O and O represent the initial and final states of disproportionation reaction of 2 OH groups, respectively. Bridge-bridge coordination is

relatively stable configuration of 2 OH radicals (Figure 2 e) and H₂O/O (Figure 2 g). Co-adsorption energy of two OH radicals is found as -6.25 eV while for H₂O/O the binding energy was -6.47 eV. Co-adsorption of OH is attractive (-0.21 eV) while that of H₂O/O is repulsive (0.26 eV).

----- **Insert Figure 2 here** -----

b. Water dissociation reactions on Au modified bimetallic surfaces

i. Water dissociation

For water dissociation, initial state (IS) refers to water adsorbed on bridge site while bridge-bridge coordination of OH and H represents the final state (FS) of dissociation products. Water has to surmount an activation barrier of 0.60 eV and is thermoneutral on the Au-Pd bimetallic model surface. At the TS, the H dissociated from H₂O occupies a bridge position, slightly bent towards OH (Figure 2 c). The corresponding barriers on Au(100) is 1.53 eV and endothermic⁶¹, while on Pd(111) the barrier is 1.05 eV.⁵³ The reduction in activation barrier and change of thermodynamics of water dissociation clearly show the beneficial effect of add-metal, a clear evidence of synergy between components of the bimetallic surface.

It is well documented fact that for actively dissociating water, bimetallic surfaces^{8,56} and metal/oxide interface⁶² play key role. It is pertinent to note here that Cu is the bench mark catalyst for water gas shift reaction. However, it suffers from a very serious drawback which is associated with its slow disintegration of water.^{63,64} The barrier reported for water dissociation on Cu(111) is 1.34 eV.¹⁵ Since water dissociation is the rate limiting step of water gas shift reaction, the barrier associated with this elementary reaction on Au (1.53 eV), Pd (1.05 eV) and Cu clearly demonstrates the importance of our results. Additionally, Knudsen et al.⁸ have modeled Cu/Pt near surface alloy and have reported a significantly high activation barrier (1.36 eV) for water dissociation than our model Pd-Au bimetallic surface. Thus, our model bimetallic surface behaves better than Au, Pd, Cu and Cu modified Pt near surface alloy.

Finally, it is necessary to quantify why presence of Pd on Au leads to lowering of barrier for the above mentioned key reaction step. For this, we calculated Bader charges⁶⁵ for clean Pd & Pd-Au bimetallic surfaces. In case of clean Pd-Au bimetallic surface, neither of the metals gains or loses charge, the charges being essentially those of bulk Pd and Au. Since upon alloy formation,

we did not observe charge redistribution, the reduction in barrier is attributable to the strain induced by the lattice mismatch. As Pd-Pd bonds are more open when alloyed with Au, thus H₂O activation may be induced by the strain, which is in line with the observations of Nakamura et al.⁶⁶ They have shown that reduction in the activation barrier for water dissociation on Cu(100) and Cu(110) is due to stretched Cu-Cu bonds which induce substrate activation and stronger Cu-hetero-atom bond formation.

ii. OH dissociation

After water dissociation, we turned to see the dissociation of OH. IS for this dissociation represents bridge coordinated OH and FS corresponds to O and H adsorbed on bridge-bridge sites. We observed that dissociation of OH requires 2.60 eV and is endothermic by 1.11 eV. OH dissociation is rather difficult and normally requires higher activation barrier than water dissociation which has been demonstrated in several recent studies.^{14,53,61,67,68}

iii. OH-OH disproportionation reaction

From the previous section we concluded that OH dissociation is not feasible, thus we examined OH-OH disproportionation reaction. For this reaction, IS refers to co-adsorbed two OH radicals on parallel bridge positions and the FS refers to O and H₂O co-adsorbed on respective bridge positions. The reaction is endothermic (0.89 eV) and has to surmount a barrier of 1.11 eV. In the TS, an H atom from one of OH groups moves to the other. At the TS, the OH bond distance increases to 1.5 Å (Figure 2 f). The TS is characterized by a unique vibrational frequency of 320.49 cm⁻¹. Similar reaction barrier has been computed on Pd-Zn and Ni-Zn bimetallic surfaces.⁶⁹ The large activation barrier and endothermic nature of OH-OH disproportionation is a direct consequence of the low activation barrier for water dissociation. Since water dissociation on this surface has to surmount a relatively smaller barrier, this suggests that any reaction leading to water formation will be difficult on this bimetallic surface.

c. CO oxidation

i. Co-adsorption of CO and O and the formation of CO₂

For formation of CO₂, CO can either react with O (the redox mechanism) or with OH (the carboxyl mechanism) forming COOH which disintegrates into CO₂ and H. We have analyzed

both of the ways for CO oxidation. In our Au-Pd bimetallic model surface, Eads of CO was -2.03 eV for bridge coordination which is comparable to that of Kim & Henkelman.⁴⁷

Following adsorption of CO, co-adsorption of CO and O was computed to complete the redox process. The adsorption energy for bridge-bridge coordination was the maximum (-6.07eV). Finally, CO₂ formation passes through formation of stable OCO complex, with a reaction barrier of 0.54 and exothermic ($\Delta H = -0.41$ eV). CO₂ desorbs from this OCO complex due to minute binding energy. Figure 2 r-u show the path for CO₂ formation from the redox mechanism.

ii. Formation and dissociation of COOH

Carboxyl mechanism involves formation of carboxyl (COOH) and its disintegration into CO₂ and H. For carboxyl formation, we first characterized the most stable binding positions of co-adsorbed CO and OH and then that of COOH. The stable co-adsorption configuration of CO-OH is the association of both CO and OH on the nearby bri positions, while COOH coordinates at bri site. Co-adsorption energy for CO-OH was found to be -4.79 eV. For formation of cis-COOH from the co-adsorbed CO-OH, an activation barrier of 0.78 eV is required. The reaction is endothermic by 0.34 eV. Cis-trans isomerization of COOH requires 0.14 eV and is downhill (-0.35 eV). CO₂ formation from COOH requires a barrier of 0.44 eV and endothermic by 0.23 eV. It is important here to note that the barrier associated with OH disproportionation is considerably larger than COOH formation. This suggests that large portion of CO will be oxidized by carboxyl path with a smaller portion to be oxidized by redox path.

d. Adsorption of 2H atoms and H₂ formation

Finally, for formation of H₂ from co-adsorbed 2H atoms, we considered co-adsorption of 2H atoms. For the adsorption of H₂, the calculations converged to dissociative adsorption of H₂ into 2H atoms. As H₂ formation is entropic driven reaction, it's not surprising that it will be produced at the operating conditions of water gas shift reaction (Temperature is approximately 525 to 573 K for low temperature shift catalysts). Formation of H₂ requires a barrier of 0.38 eV on this bimetallic surface. Dissociative adsorption of H₂ has also been demonstrated very recently on Au-Pd(111) disordered alloy.⁷⁰

H₂ is a stable molecule and hardly interacts with most of the materials' surfaces. Its inert behavior makes its decomposition and storage a very difficult task. Therefore, it is stored in cost effective liquid form. As the adsorption of the H₂ is dissociative on this model bimetallic surface, and that H₂ formation is entropic driven reaction. Thus a thermally induced desorption process will produce H₂ gas, owing to the small barrier (0.38 eV) associated with H₂ formation. This suggests that Pd-Au bimetallic surface could be potential candidate for hydrogen storage material.

4. Discussion

Figure 3. shows the potential energy diagram for two competing reactions for water gas shift reaction. As abstraction of H from OH requires substantially large activation energy, this reaction is difficult to occur on Au-Pd system. Although, disproportionation of OH radicals also requires large barrier, nevertheless, it will be competing with carboxyl formation in practical situations. Depending upon activation barriers of disproportionation of OH radicals and the carboxyl formation, it seems that carboxyl pathway will dominate the redox process on this surface, consistent with experimental and theoretical predictions confirming the carboxyl to be the potential intermediate for CO oxidation in shift reaction.^{14,61,71-74}

----- **Insert Figure 3 here** -----

It is interesting here to compare barrier for H₂O dissociation and CO oxidation by atomic O to realize any beneficial effect of Pd on Au. Compared to Au-Pd bimetallic surface, the corresponding barriers for H₂O dissociation on Au(100) is 1.53 eV⁶¹, while on Pd(111) the barrier is 1.05 eV.⁵³ Similarly, CO oxidation by atomic O also shows significant reduction in activation barrier upon construction of Au-Pd bimetallic surface. The barrier is 0.54 and exothermic ($\Delta H = -0.41$ eV), versus 0.90 and 1.06 on Pd(100)^{75,76} and 0.68 on Au(221).⁷⁷ Thus, a beneficial effect of Pd on Au is demonstrated in H₂O dissociation and subsequent CO oxidation. As far as the life span of Pd-O is concerned, Kim & Henkelman⁴⁷ have shown that although, PdO formation may be computed by DFT calculations, but in real operating conditions, formation of PdO is hard to take place. This leads us to conclude that Pd-Au bimetallic surface provide a very good alternative catalyst for H₂O dissociation as well as for CO oxidation. Although, actual active sites in Au-Pd catalyst may differ from our model surface, still we are

convinced that a cooperative effect between Au-Pd would be beneficial for CO oxidation and H₂O dissociation. Moreover, very recently, Kim & Henkelman⁴⁷ have shown that for Pd motifs larger than 4, the overall CO oxidation reactivity of Pd-Au will be that of the pure Pd(100) surface, therefore, it is expected that the maximum synergic effect of Au-Pd will be limited to the monolayer of Pd on Au.

To sum up, we present here brief overview of synergy between the component metals for different reactions. A strong promotional effect has been observed for Cu-Pt near surface alloy for shift reaction by Knudsen et al.⁸ They have shown that the adsorption of reaction products is weaker and that the alloy is stable towards CO induced segregation. Similarly, it was observed that the oxidation of Ni based anodes can be enhanced by creating a bimetallic surface for solid oxide fuel cells. Particularly Ni based bimetallic surfaces consisting of Cu, Fe or Co were shown to be most active surfaces for anode oxidation.⁷⁸ A synergy between Cu/Fe is suggested to operate in higher alcohol synthesis (HAS) making the bimetallic surface more active for higher alcohol synthesis (HAS).⁴⁸ Fajín et al.⁵⁶ have observed that for adsorption, dissociation and stabilization of dissociation products of water, bimetallic surfaces had a cooperative effect between the components. The activation barrier for H abstraction from H₂O is significantly smaller on the bimetallic surface than the monometallic parts, showing a synergy between the two metals. Several classical examples can be given in which the bimetallic surfaces performed superior to the counterpart monometallic surfaces. Interested readers can have look on these articles.^{36,48,79–83} Similarly, synergy between Au-Pd has been shown in a number of reactions. We have given a brief overview of Au-Pd alloy used in some of chemical process in Introduction section. A classic review⁸⁴, aims at discussing the synergy between component metals of a bimetallic alloy for catalysis; several examples of catalysis over Au-Pd nanoalloy can be found in this review, originating from synergy between Au-Pd.

From the above discussion, it's quite convincing that presence of Pd on Au alters the catalytic performance of surface. Both the H₂O dissociation and CO oxidation are much more easily carried out on the bimetallic surface than either of the counterpart surfaces, a clear indication of synergy between Au-Pd. As the components of an alloy have distinct atomic arrangements, therefore, metal-metal interactions not only tune the bonding between the catalyst surface and the reactants but also provide extra stabilization to the transition state which is an additional benefit of synergy.

5. Conclusion

Density Functional Theory calculations were performed to model a reaction relevant bimetallic surface and study water gas shift reaction. Thermodynamically, in vacuum, Pd prefers to stay in the bulk due to more negative formation energies. However, strong CO-phillic nature of Pd causes surface segregation of Pd atoms, with segregation energy increasing linearly with number of Pd atoms segregated. While Pd-Pd bonds formation both in surface and subsurface layer is inhibited in vacuum, CO induces Pd-Pd bond formation, which indicates that under CO rich environments, Pd covered Au will be the could be a relevant structure of the Pd-Au bimetallic surface. The surface is highly active for water dissociation and subsequent reactions leading to CO oxidation. On the basis of activation barrier, we conclude that the adsorbed carboxyl pathway will be the dominant reaction mechanism. Our results show that H₂ adsorbs dissociatively on this surface which indicates that the surface could be a suitable material for hydrogen storage. An important consequence of our results is that these guide into selective development of alloy surfaces keeping in view the adsorbate induced surface segregations.

6. Acknowledgement

Author AAL highly acknowledges the support of Brazilian agencies FAPEMIG (CEX PPM 00262/13), CAPES and CNPq.

7. Supporting information

8. References

- 1 V. Subramani and S. K. Gangwal, *Energy & Fuels*, 2008, **22**, 814–839.
- 2 M. Z. Jacobson, W. G. Colella and D. M. Golden, *Science (80-.)*, 2005, **308**, 1901–1905.
- 3 W. Wang, S. Wang, X. Ma and J. Gong, *Chem. Soc. Rev.*, 2011, **40**, 3703–3727.
- 4 J. J. Spivey, *Catal. today*, 2005, **100**, 171–180.
- 5 J. Greeley and M. Mavrikakis, *Nat. Mater.*, 2004, **3**, 810–815.
- 6 K. Nishida, I. Atake, D. Li, T. Shishido, Y. Oumi, T. Sano and K. Takehira, *Appl. Catal. A Gen.*, 2008, **337**, 48–57.
- 7 X. Zhao, S. Ma, J. Hrbek and J. A. Rodriguez, *Surf. Sci.*, 2007, **601**, 2445–2452.

- 8 J. Knudsen, A. U. Nilekar, R. T. Vang, J. Schnadt, E. L. Kunkes, J. A. Dumesic, M. Mavrikakis and F. Besenbacher, *J. Am. Chem. Soc.*, 2007, **129**, 6485–6490.
- 9 A. Hussain, *J. Phys. Chem. C*, 2013, **117**, 5084–5094.
- 10 D. Zhao and B.-Q. Xu, *Angew. Chemie Int. Ed.*, 2006, **45**, 4955–4959.
- 11 B. Hammer and J. K. Nørskov, *Adv. Catal.*, 2000, **45**, 71–129.
- 12 M. Haruta, T. Kobayashi, H. Sano and N. Yamada, *Chem. Lett.*, 1987, 405–408.
- 13 M. Haruta, N. Yamada, T. Kobayashi and S. Iijima, *J. Catal.*, 1989, **115**, 301–309.
- 14 A. Hussain, J. Gracia, B. E. Nieuwenhuys and J. W. Niemantsverdriet, *ChemCatChem*, 2013, **5**, 2479–2488.
- 15 A. A. Gokhale, J. A. Dumesic and M. Mavrikakis, *J. Am. Chem. Soc.*, 2008, **130**, 1402–1414.
- 16 A. E. Baber, H. L. Tierney and E. C. H. Sykes, *ACS Nano*, 2010, **4**, 1637–1645.
- 17 D. W. Yuan and Z. R. Liu, *Phys. Lett. A*, 2011, **375**, 2405–2410.
- 18 B. E. Koel, A. Sellidj and M. T. Paffett, *Phys. Rev. B*, 1992, **46**, 7846–7856.
- 19 S. Ogura, M. Okada and K. Fukutani, *J. Phys. Chem. C*, 2013, **117**, 9366–9371.
- 20 Y.-F. Han, J.-H. Wang, D. Kumar, Z. Yan and D. W. Goodman, *J. Catal.*, 2005, **232**, 467–475.
- 21 M. S. Chen, K. Luo, T. Wei, Z. Yan, D. Kumar, C.-W. Yi and D. W. Goodman, *Catal. today*, 2006, **117**, 37–45.
- 22 D. Kumar, M. S. Chen and D. W. Goodman, *Catal. Today*, 2007, **123**, 77–85.
- 23 D. I. Enache, J. K. Edwards, P. Landon, B. Solsona-Espriu, A. F. Carley, A. A. Herzing, M. Watanabe, C. J. Kiely, D. W. Knight and G. J. Hutchings, *Science (80-.)*, 2006, **311**, 362–365.
- 24 H. C. Ham, G. S. Hwang, J. Han, S. W. Nam and T. H. Lim, *J. Phys. Chem. C*, 2009, **113**, 12943–12945.
- 25 J. Xu, T. White, P. Li, C. He, J. Yu, W. Yuan and Y.-F. Han, *J. Am. Chem. Soc.*, 2010, **132**, 10398–10406.
- 26 F. Gao, Y. Wang and D. W. Goodman, *J. Phys. Chem. C*, 2009, **113**, 14993–15000.

- 27 F. Gao, Y. Wang and D. W. Goodman, *J. Am. Chem. Soc.*, 2009, **131**, 5734–5735.
- 28 M. H. Shao, T. Huang, P. Liu, J. Zhang, K. Sasaki, M. B. Vukmirovic and R. R. Adzic, *Langmuir*, 2006, **22**, 10409–10415.
- 29 Y. Xing, Y. Cai, M. B. Vukmirovic, W.-P. Zhou, H. Karan, J. X. Wang and R. R. Adzic, *J. Phys. Chem. Lett.*, 2010, **1**, 3238–3242.
- 30 C.-W. Yi, K. Luo, T. Wei and D. W. Goodman, *J. Phys. Chem. B*, 2005, **109**, 18535–18540.
- 31 Z. Li, O. Furlong, F. Calaza, L. Burkholder, H. C. Poon, D. Saldin and W. T. Tysoe, *Surf. Sci.*, 2008, **602**, 1084–1091.
- 32 T. V. de Bocarmé, M. Moors, N. Kruse, I. S. Atanasov, M. Hou, A. Cerezo and G. D. W. Smith, *Ultramicroscopy*, 2009, **109**, 619–624.
- 33 V. Soto-Verdugo and H. Metiu, *Surf. Sci.*, 2007, **601**, 5332–5339.
- 34 B. Lim, H. Kobayashi, T. Yu, J. Wang, M. J. Kim, Z.-Y. Li, M. Rycenga and Y. Xia, *J. Am. Chem. Soc.*, 2010, **132**, 2506–2507.
- 35 G. Maire, L. Hilaire, P. Legare, F. G. Gault and A. O’cinneide, *J. Catal.*, 1976, **44**, 293–299.
- 36 G. Zanti and D. Peeters, *J. Phys. Chem. A*, 2010, **114**, 10345–10356.
- 37 G. Kresse and J. Furthmüller, *Comput. Mater. Sci.*, 1996, **6**, 15–50.
- 38 G. Kresse and J. Furthmüller, *Phys. Rev. B*, 1996, **54**, 11169.
- 39 P. E. Blöchl, *Phys. Rev. B*, 1994, **50**, 17953.
- 40 J. P. Perdew and Y. Wang, *Phys. Rev. B*, 1992, **45**, 13244.
- 41 J. P. Perdew, J. A. Chevary, S. H. Vosko, K. A. Jackson, M. R. Pederson, D. J. Singh and C. Fiolhais, *Phys. Rev. B*, 1992, **46**, 6671.
- 42 H. J. Monkhorst and J. D. Pack, *Phys. Rev. B*, 1976, **13**, 5188.
- 43 M. Methfessel and A. T. Paxton, *Phys. Rev. B*, 1989, **40**, 3616.
- 44 G. Henkelman, B. P. Uberuaga and H. Jónsson, *J. Chem. Phys.*, 2000, **113**, 9901–9904.
- 45 G. Henkelman and H. Jonsson, *J. Chem. Phys.*, 2000, **113**, 9978–9985.

- 46 J. D. Head, *Int. J. Quantum Chem.*, 1997, **65**, 827–838.
- 47 H. Y. Kim and G. Henkelman, *ACS Catal.*, 2013, **3**, 2541–2546.
- 48 Y. Zhao, S. Li and Y. Sun, *J. Phys. Chem. C*, 2013, **117**, 24920–24931.
- 49 M. Sansa, A. Dhouib and H. Guesmi, *J. Chem. Phys.*, 2014, **141**, 64709.
- 50 S. A. Tenney, J. S. Ratliff, C. C. Roberts, W. He, S. C. Ammal, A. Heyden and D. A. Chen, *J. Phys. Chem. C*, 2010, **114**, 21652–21663.
- 51 R. C. Weast, M. J. Astle and W. H. Beyer, 1988.
- 52 M. Pozzo, G. Carlini, R. Rosei and D. Alfè, *J. Chem. Phys.*, 2007, **126**, 164706.
- 53 A. A. Phatak, W. N. Delgass, F. H. Ribeiro and W. F. Schneider, *J. Phys. Chem. C*, 2009, **113**, 7269–7276.
- 54 R. R. Q. Freitas, R. Rivelino, F. de Brito Mota and C. M. C. de Castilho, *J. Phys. Chem. C*, 2012, **116**, 20306–20314.
- 55 L.-Y. Gan, R.-Y. Tian, X.-B. Yang, H.-D. Lu and Y.-J. Zhao, *J. Phys. Chem. C*, 2011, **116**, 745–752.
- 56 J. L. C. Fajín, M. N. D. S. Cordeiro and J. R. B. Gomes, *J. Phys. Chem. C*, 2012, **116**, 10120–10128.
- 57 R.-J. Lin, H.-L. Chen, S.-P. Ju, F.-Y. Li and H.-T. Chen, *J. Phys. Chem. C*, 2012, **116**, 336–342.
- 58 C. A. Farberow, A. Godinez-Garcia, G. Peng, J. F. Perez-Robles, O. Solorza-Feria and M. Mavrikakis, *ACS Catal.*, 2013, **3**, 1622–1632.
- 59 J. L. C. Fajín, A. Bruix, M. N. D. S. Cordeiro, J. R. B. Gomes and F. Illas, *J. Chem. Phys.*, 2012, **137**, 34701.
- 60 M. Hu, D. P. Linder, M. Buongiorno Nardelli and A. Striolo, *J. Phys. Chem. C*, 2013, **117**, 15050–15060.
- 61 P. Liu and J. A. Rodriguez, *J. Chem. Phys.*, 2007, **126**, 164705.
- 62 K. Mudiyansele, S. D. Senanayake, L. Feria, S. Kundu, A. E. Baber, J. Graciani, A. B. Vidal, S. Agnoli, J. Evans, R. Chang, S. Axnanda, Z. Liu, J. F. Sanz, P. Liu, J. A. Rodriguez and D. J. Stacchiola, *Angew. Chemie Int. Ed.*, 2013, **52**, 5101–5105.

- 63 S. D. Senanayake, J. T. Sadowski, J. Evans, S. Kundu, S. Agnoli, F. Yang, D. Stacchiola, J. I. Flege, J. Hrbek and J. A. Rodriguez, *J. Phys. Chem. Lett.*, 2012, **3**, 839–843.
- 64 S. Yamamoto, K. Andersson, H. Bluhm, G. Ketteler, D. E. Starr, T. Schiros, H. Ogasawara, L. G. M. Pettersson, M. Salmeron and A. Nilsson, *J. Phys. Chem. C*, 2007, **111**, 7848–7850.
- 65 R. F. W. Bader, *Atoms in molecules*, Wiley Online Library, 1990.
- 66 J. Nakamura, J. M. Campbell and C. T. Campbell, *J. Chem. Soc., Faraday Trans.*, 1990, **86**, 2725–2734.
- 67 L. Yang, A. Karim and J. T. Muckerman, *J. Phys. Chem. C*, 2013, **117**, 3414–3425.
- 68 C.-H. Lin, C.-L. Chen and J.-H. Wang, *J. Phys. Chem. C*, 2011, **115**, 18582–18588.
- 69 H. Wei, C. Gomez and R. J. Meyer, *Top. Catal.*, 2012, **55**, 313–321.
- 70 N. Takehiro, P. Liu, A. Bergbreiter, J. K. Nørskov and R. J. Behm, *Phys. Chem. Chem. Phys.*, 2014, **16**, 23930–23943.
- 71 F. C. Meunier, A. Goguet, C. Hardacre, R. Burch and D. Thompsett, *J. Catal.*, 2007, **252**, 18–22.
- 72 F. C. Meunier, D. Reid, A. Goguet, S. Shekhtman, C. Hardacre, R. Burch, W. Deng and M. Flytzani-Stephanopoulos, *J. Catal.*, 2007, **247**, 277–287.
- 73 F. C. Meunier, D. Tibiletti, A. Goguet, S. Shekhtman, C. Hardacre and R. Burch, *Catal. Today*, 2007, **126**, 143–147.
- 74 S. D. Senanayake, D. Stacchiola, P. Liu, C. B. Mullins, J. Hrbek and J. A. Rodriguez, *J. Phys. Chem. C*, 2009, **113**, 19536–19544.
- 75 B. Hammer, *J. Catal.*, 2001, **199**, 171–176.
- 76 P. Salo, K. Honkala, M. Alatalo and K. Laasonen, *Surf. Sci.*, 2002, **516**, 247–253.
- 77 Z.-P. Liu, P. Hu and A. Alavi, *J. Am. Chem. Soc.*, 2002, **124**, 14770–14779.
- 78 W. An, D. Gatewood, B. Dunlap and C. H. Turner, *J. Power Sources*, 2011, **196**, 4724–4728.
- 79 Y. Shiraishi, H. Sakamoto, Y. Sugano, S. Ichikawa and T. Hirai, *ACS Nano*, 2013, **7**, 9287–9297.

- 80 C. Wang, D. Van der Vliet, K. L. More, N. J. Zaluzec, S. Peng, S. Sun, H. Daimon, G. Wang, J. Greeley and J. Pearson, *Nano Lett.*, 2010, **11**, 919–926.
- 81 C. Song, Q. Ge and L. Wang, *J. Phys. Chem. B*, 2005, **109**, 22341–22350.
- 82 K. Koszinowski, D. Schröder and H. Schwarz, *J. Am. Chem. Soc.*, 2003, **125**, 3676–3677.
- 83 R. Ferrando, J. Jellinek and R. L. Johnston, *Chem. Rev.*, 2008, **108**, 845–910.
- 84 H.-L. Jiang and Q. Xu, *J. Mater. Chem.*, 2011, **21**, 13705–13725.

-----Tables and Figures-----

Table 1. Adsorption energies, M-A distance and surface relaxation (or contraction) are listed. All the distances are in angstroms while energies are in electron volts.

Species	Ads. site	E_{ads}	$d_{\text{M-A}}$	Lateral relaxation	Vertical relaxation
H₂O	Top	-0.33	2.38	0.04	0.02
	Bri	-0.27	2.45		
OH	Bri	-2.84	2.08		
	Hol	-3.02	2.33	0.03	-0.03
H	Bri	-2.81	1.72	-0.06	0.02
	Hol	-2.66	1.96		
O	Bri	-4.13	1.94		

	Hol	-4.39	2.17	-0.12	
OH + H	Bri-bri	-5.81	2.11, 1.71	0.18, 0	0.08, 0.02
O + H	bri-bri	-6.61	1.99, 1.72	0.07, -0.04	0.11, 0.06
OH + OH	Bri-bri	-6.26	2.14, 2.09	0.20, 0.20	0.10, 0.10
H₂O + O	Bri-bri	-4.47	2.22, 1.95	0.43, 0.23	0.07, 0.11
CO	Bri	-2.02	2.08	0.32	0.12
	hol	-1.88			
CO + OH			2.0, 2.09	-0.06, 0.29	0.7, 0.14
CO + O	Bri-bri	-6.07	1.95, 1.89	0.27, 0.05	0.3, 0.14
H + H	Bri-bri	-5.61	1.71, 1.74	-0.03, -0.03	0.03, 0.03

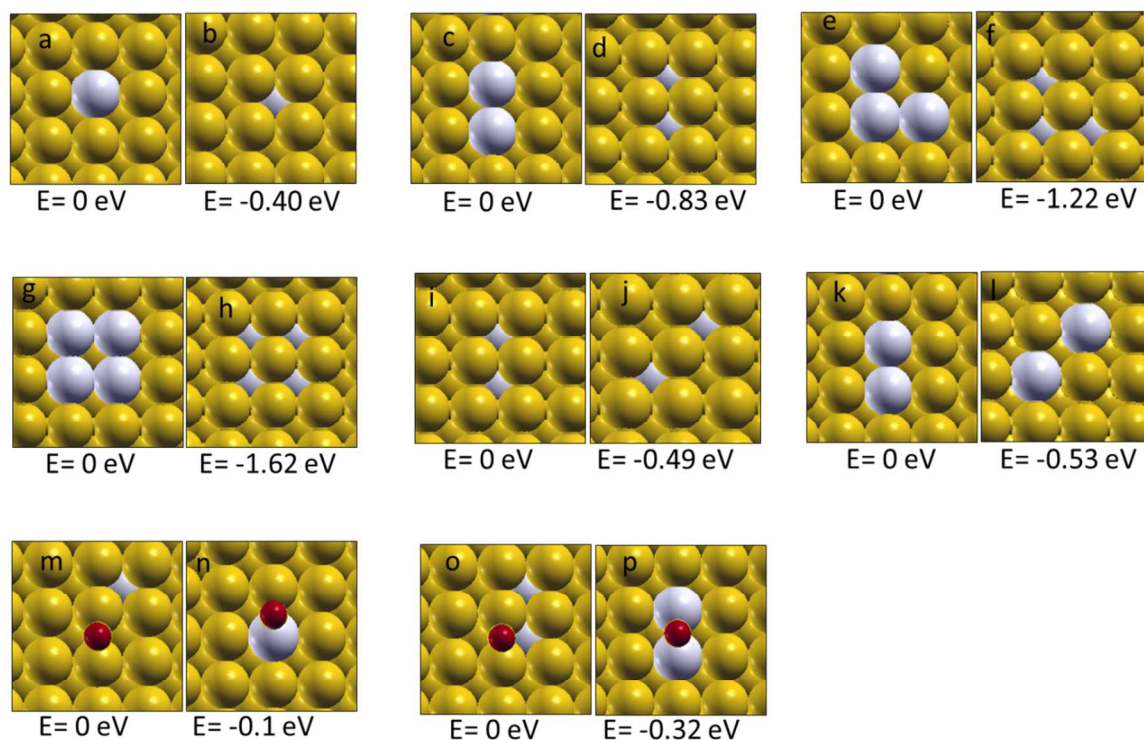


Figure 1 Relative energy of segregation of 1 (a,b), 2 (c,d), 3 (e,f) and 4 (g,h) atoms from subsurface to surface layer, formation of Pd dimer on the subsurface layer (i,j) and surface layer (k,l) and CO induced segregation of 1(m,n) and 2 Pd (o,p) atoms. Yellow and white balls indicate Au and Pd, respectively. Parts a to h show linear increase in the relative segregation energies when number of Pd atoms increase from 1 to 4. The systems are significantly stabilized when Pd go in sub-surface region. Additionally, system becomes more stable (k & l) when Pd atoms are placed at diagonal positions instead of adjacent sites to form dimer in the top layer. However, when CO is adsorbed, situation reverses as indicated in parts m to p.

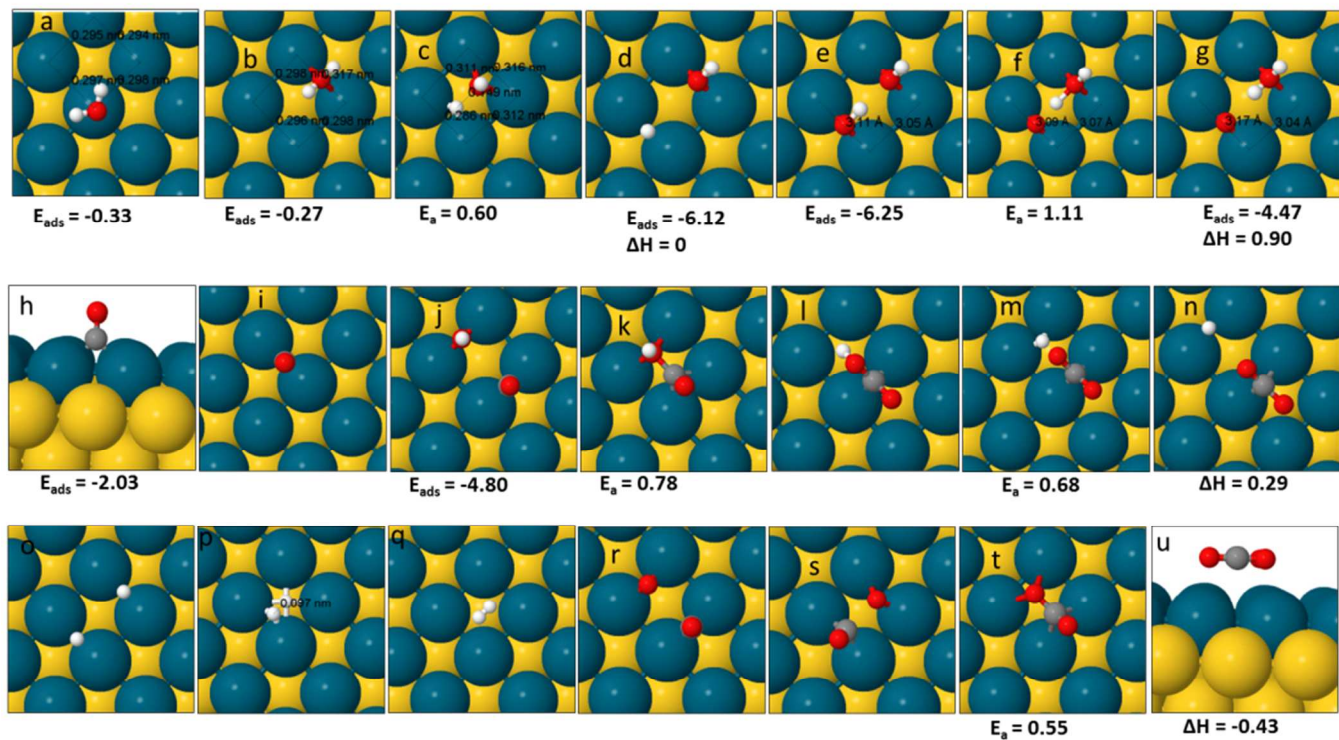


Figure 2 Adsorption configurations of reactants, transition states and products of elementary reactions involved in water gas shift reaction on PdAu bimetallic surface.

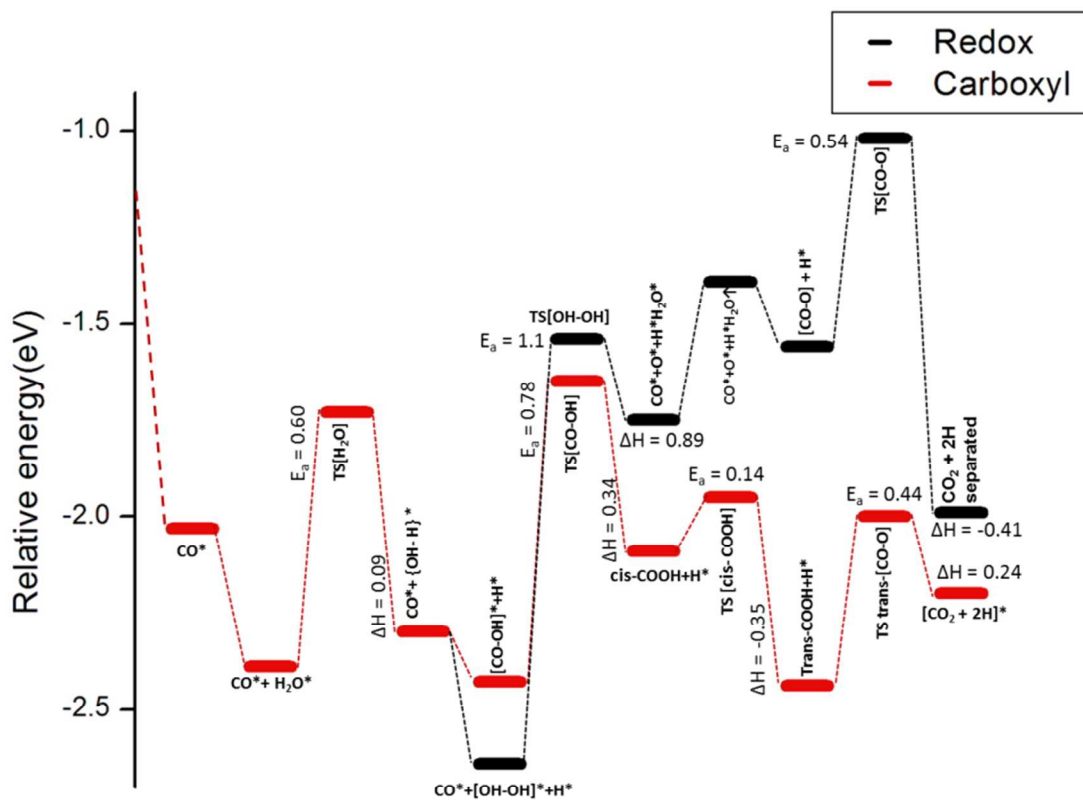


Figure 3 Potential energy diagram for redox and carboxyl mechanism on Pd-Au bimetallic surface.